Journal of Oceanology and Limnology
Vol. 40 No. 3, P. 1148-1159, 2022
https://doi.org/10.1007/s00343-021-1141-7

Cytological and transcriptional analysis reveal phosphatidylinositol signaling pathway plays key role in mitotic division of *Pyropia yezoensis**

Yunke ZHU[1], Xinran WANG[1], Bin SUN[1], Xianghai TANG[1, **], Yunxiang MAO[2, 3, **]

[1] *Key Laboratory of Marine Genetics and Breeding* (*Ministry of Education*), *College of Marine Life Sciences*, *Ocean University of China*, *Qingdao 266003*, *China*

[2] *MOE Key Laboratory of Utilization and Conservation for Tropical Marine Bioresources*, *College of Fisheries and Life Science*, *Hainan Tropical Ocean University*, *Sanya 572022*, *China*

[3] *Laboratory for Marine Biology and Biotechnology*, *Pilot National Laboratory for Marine Science and Technology* (*Qingdao*), *Qingdao 266237*, *China*

Received Apr. 23, 2021; accepted in principle May 19, 2021; accepted for publication Jun. 18, 2021

Abstract The phosphatidylinositol (PI) signaling system, a central regulator of eukaryotic metabolism, is widely found in eukaryotes for regulating a variety of cell activities. Most of the genes in the PI signaling system were found conserved in *Pyropia yezoensis*. In this experiment, wortmannin was used as an inhibitor to inhibit the activity of phosphatidylinositol-3 kinase (*PI3K*), an important regulator of the PI signaling system. After wortmannin treatment, the mitotic division of *P. yezoensis* was significantly inhibited in a dose-dependent manner, and the mitotic division percentage was reduced by 68.1% and 91.9% in the 5- and 10-μmol/L groups, respectively. When thalli were treated with wortmannin, the levels of reactive oxygen species (ROS) were significantly decreased. Furthermore, the expression level of *PI3K* was inhibited and the expression levels of downstream genes regulated by *PI3K* was significantly changed. In the *PI3K-AGC* signaling pathway, the expression levels of Serine/threonine protein kinase (*AGC*) and cyclin-dependent kinases A (*CDKA*) were downregulated, while WEE1 kinase gene (*WEE1*) was upregulated. Three nicotinamide adenine dinucleotide phosphate (NADPH) oxidase genes were downregulated after wortmannin treatment. These results indicate that the PI signaling system plays an important role in the regulation of cell activity in *P. yezoensis*. It was speculated that the growth and development of *P. yezoensis* might be regulated by *P. yezoensis PI3K*, which promoted the expression of the *AGC* gene and further regulates the expression of downstream *WEE1* and *CDKA* genes to advance mitotic division, and also promoted the expression level of NADPH oxidase that regulates ROS homeostasis.

Keyword: *Pyropia yezoensis*; phosphatidylinositol signaling system; reactive oxygen species; mitotic division

Abbreviation: PI: phosphatidylinositol; $InsP_3$: inositol (1,4,5)-trisphosphate; PI-PLC: phosphoinositide-specific phospholipase C; ROS: reactive oxygen species; *PI3K*: phosphatidylinositol-3 kinase; *PI4K*: phosphatidylinositol 4-kinase; *PIP5K*: phosphatidylinositol-4-phosphate 5-kinase; NOX: nicotinamide adenine dinucleotide phosphate (NADPH) oxidase; EdU: 5-ethynyl-20-deoxyuridine; DCFH-DA: 2,7-dichlorodi-hydrofluorescein diacetate

1 INTRODUCTION

Similar to other eukaryotes, the plant phosphatidylinositol (PI) signaling system is a complex network that participates in the regulation of key physiological processes essential to plant function

* Supported by the National Key R&D Program of China (Nos. 2018YFD0900106, 2020YFD0901101), the Marine S&T Fund of Shandong Province for Pilot National Laboratory for Marine Science and Technology (Qingdao) (No. 2018SDKJ0302-4), the Fundamental Research Funds for the Central Universities (No. 202064006), the MOA Modern Agricultural Talents Support Project, and Special Project of Central Government Guiding Local Science and Technology Development (No. 7033204020)
** Corresponding authors: txianghai@ouc.edu.cn; yxmao@hntou.edu.cn

and development. At present, inositol phospholipids, inositol phosphates, and related enzymes of the PI signaling system have been identified in plant cell nuclei (Dieck et al., 2012). Inositol 1,4,5-trisphosphate ($InsP_3$), regulated by inositol polyphosphate 5-phosphatase, can induce the release of calcium ions and is crucial for maintaining pollen dormancy, regulating the early germination of pollen, and closure of stomata (Wang et al., 2012). In addition, evidence showed that inositol polyphosphate 5-phosphatase participated in the control of cell division direction, cell wall pectin deposition, and actin organization, essential for the formation of internode meristems (Sato-Izawa et al., 2012). The PI signaling system also plays a role in the regulation of DNA synthesis. In soybean cells, the inhibitory effect of the chemical inhibitor U-73122 on phosphoinositide-specific phospholipase C (PI-PLC) activity reduces $InsP_3$ content, resulting in a reduction in the DNA synthesis rate by more than 30% (Shigaki and Bhattacharyya, 2002). In *Arabidopsis*, phosphatidylinositol-4-phosphate 5-kinase (*PIP5K*) is highly expressed in specialized meristems and is involved in the control of cell proliferation, similar to that in animals and yeast (Elge et al., 2001).

Previous studies have shown that phosphatidylinositol-3 kinase (*PI3K*) plays an important role in cell cycle regulation, development, and signal transduction by participating in endocytosis, reactive oxygen species (ROS) production, and transcriptional activity (Marqués et al., 2009; Lee et al., 2010; Campa et al., 2015). In *Chlamydomonas reinhardtii*, the inhibition or knockdown of *PI3K* significantly decreased the cell growth, changed the cell morphology, and increased the fat and starch contents (Ramanan et al., 2018). In wheat, *PI3K* inhibitor treatment could inhibit the root growth of germinated seeds, reduce the mitotic index, and affect the structure and function of the meristemic nucleolus (Ni and Zhang, 2014). In animals, the role of *PI3K* in regulating the timing of cell division through the cell cycle progression rate has been widely confirmed (Alvarez et al., 2003; Dangi et al., 2003; Campa et al., 2015). *PI3K*-dependent signaling regulates mammalian cell proliferation by promoting the G1/S and G2/M phases of the cell cycle. The inhibition of *PI3K* decreased the cyclinB1 expression, cell division cycle 2 (*CDC2*) activity, and the mitotic index (Dangi et al., 2003). Studies have shown that the *PI3K*-*AGC* pathway positively regulated the cell cycle at the G2/M boundary, which might be accomplished by regulating the expression of WEE1 kinase gene (*WEE1*) and the modification of *CDC2* (Katayama et al., 2005; Wu et al., 2018; Xu et al., 2018). Furthermore, *PI3K* participated in the production of ROS by producing phosphatidylinositol 3-phosphate (PtdIns(3)P) (Joo et al., 2005). As the second messenger of plant hormone signals, ROS regulates a variety of biological processes, such as seed germination, seedling growth, root gravitation, apical growth, and programmed cell death (Garg and Manchanda, 2009; Hakeem et al., 2014). Changes in ROS distribution could alter the stability of PLETHORA2 (*PLT2*) protein, thereby regulating the root stem cell niche (Yamada et al., 2020). Nicotinamide adenine dinucleotide phosphate (NADPH) oxidase is the primary source of ROS production, and could catalyzes the production of O^{2-} and regulates a wide range of biological functions in different organisms (Kaur and Pati, 2016). NADPH oxidase deficiency in *Arabidopsis thaliana* root hair defective 2 (*rhd2*) mutant impaired cell expansion, and the resulting mutant has short root hair and dysplastic roots (Foreman et al., 2003). In plants, *PI3K* has been demonstrated to change the quantity of reactive oxygen species by regulating the expression and activity of NADPH oxidase (Lee et al., 2008; Liu et al., 2012; Livanos et al., 2012).

Pyropia yezoensis is a representative species of Bangiales (Rhodophyta), which grows naturally in the intertidal zone. Some species of *Pyropia* have been industrially cultivated on a large scale because of their high economic value, particularly along the East Asian coast (Blouin et al., 2011). The analysis of the growth, development, and environmental adaptation of *P. yezoensis* will help in the development of methods to increase its yield, allowing for greater economic benefits. In *P. yezoensis*, *PI3K* participates in the asymmetric migration of F-actin, which is necessary for the establishment of cell polarity (Li et al., 2008). The role of ROS in biological and abiotic responses in *P. yezoensis* has been demonstrated (Tang et al., 2019).

PI3K may play an important role in regulating cell division and ROS production in *P. yezoensis*, but this aspect has not yet been extensively investigated. In this study, the thalli of *P. yezoensis* were treated with wortmannin, which has been widely used to study *PI3K* function in seed germination, root growth, and vesicle transport. Subsequently, the cell status, mitotic division, and ROS levels of the thalli were evaluated. The expression changes of the *PI3K*, Serine/threonine protein kinase (*AGC*), *WEE1*, *CDKA* (*CDC2* homologous gene), and 4 NADPH oxidase genes

after wortmannin treatment, were also detected. The importance of the PI signaling pathway in regulating mitotic division and ROS homeostasis in *P. yezoensis* is discussed in detail.

2 MATERIAL AND METHOD

2.1 Materials and reagent

A lab-cultured pure line RiZhai (RZ) of *P. yezoensis* was used for experiment. Gametophytic thalli (approximately 5 cm) were aerobically cultivated in 500-mL flasks containing sterile seawater with PES (Provasoli's Enriched Seawater Medium/Provasoli's ES Medium) medium at 10 °C, photoperiod 12-h L: 12-h D, and a light intensity of 40 μmol photons/(m^2·s). The culture medium was renewed every 3 d during the cultivation process.

Wortmannin is a fungal metabolite that is used as a highly selective *PI3K* inhibitor. It has no inhibitory effect on Ptdlns-4-kinase, protein kinase C, or phosphoinositide-specific phospholipase C (PI-PLC) (Powis et al., 1994). At present, wortmannin is widely used in the study of *PI3K* function in seed germination, root growth, and vesicle transport.

5-ethynyl-20-deoxyuridine (EdU) is a nucleotide analogue of thymidine that is incorporated into DNA during the S-phase of DNA synthesis (Fujinami et al., 2017). In the present study, the iClick™ EdU Alexa Fluor™ 488 Imaging Kit was used to characterize the percentage of cell division.

Similarly, ROS were detected using an ROS assay kit (S0033S; Beyotime). As a fluorescent probe, 2,7-dichlorodi-hydrofluorescein diacetate (DCFH-DA) has no fluorescence itself and can freely cross the cell membrane because of its extremely strong lipophilicity. After entering the cell, it is hydrolyzed by esterase and forms polar dichlorofluorescin (DCFH), which is oxidized by ROS to dichlorofluorescein (DCF), which cannot penetrate the cell membrane, and has strong green fluorescence. DCF formation was directly proportional to the level of intracellular ROS. Thus, the fluorescence intensity of DCF, detected by fluorescence microscopy, represents the level of intracellular ROS (Rastogi et al., 2010; Aranda et al., 2013).

2.2 Identification and analysis of PI signaling system genes and NADPH oxidase genes in *P. yezoensis*

The genome of *P. yezoensis* was used as the reference genome (DDBJ/ENA/GenBank: GCA_009829735.1). Gene annotation of the genes mentioned in this article was generated according to genomic annotation results of the pure line RZ of *P. yezoensis* (Wang et al., 2020). Software Snapgene was used to predict the relative molecular weights (Mw) and isoelectric points (pI) of the PI3K protein. The secondary structure of the PI3K protein was predicted using the NPS online service (http://npsa-pbil.ibcp.fr/cgi-bin/npsa_automat.pl?page=npsa_sopma.html). The homologous protein sequences of the *PI3K* gene in other species were searched and downloaded from the NCBI database (https://www.ncbi.nlm.nih.gov/). Software ClustalX was used to perform multiple sequence alignments using the full-length amino acid sequence of the *PI3K* gene. The maximum likelihood (ML) tree was constructed using the Poisson model with the MEGA-X tool, and 1 000 bootstrap replications were used to assess the reliability of the branches. The conserved domains of 11 NADPH oxidase proteins were searched using the NCBI Conserved Domains Database (CDD) Batch search (https://www.ncbi.nlm.nih.gov/), and TBtools were used for visual analysis (Chen et al., 2020). PlantCARE (http://bioinformatics.psb.ugent.be/webtools/plantcare/html/) was used to predict and analyze the action elements in the promoter region 2 000 bp before the transcription start site of 11 NADPH oxidase genes.

2.3 Cell status and viability detection

Thalli were placed in a 24-well plate. Sterile seawater (2 mL) supplemented with PES was added to each well, and the concentrations of wortmannin were adjusted to 0, 5, and 10 μmol/L, and cultured for 3 d. After 3 d, cell morphology was observed using bright field microscopy, and cell autofluorescence was observed at an excitation light of 450–490 nm, 528–553 nm, and 330–380 nm using a fluorescence microscope. The photosynthetic parameters of thalli were detected using the chlorophyll fluorescence imaging system FluorCAM MF800 and were analyzed by one-way analysis of variance (ANOVA) using SPSS software. After staining with 0.04% trypan blue dye solution (dissolved in sterile seawater) for 3 min, cell viability was detected using a microscope.

2.4 Mitotic division measure

Thalli were cultured in a 24-well plate, and the wortmannin concentrations were adjusted to 0, 5, and

10 μmol/L. Then, 20-μmol/L EdU, a thymine analogue, was added and the cells were cultured for 4 d. Immobilization, penetration, and staining were performed according to the iClick™ EdU Alexa Fluor™ 488 Imaging Kit instructions. Mitotic division was observed under 488-nm excitation light using a fluorescence microscope. Three random fields in the middle part of the thalli were selected for counting, and each concentration contained three biological replicates. Mitotic division percentage was calculated as follows:

Mitotic division percentage=(EdU-labelled cells/ total number of cells)×100%.

Software Imaris was used for cell counting, and software Photoshop CC was used for image processing. Mitotic division percentage was analyzed by ANOVA using software SPSS.

2.5 Reactive oxygen species assay

ROS in the thalli were detected using an ROS assay kit (S0033S; Beyotime). The procedure for ROS detection in situ was as follows: thalli were cultured in 24-well plates with 0-, 5-, and 10-μmol/L wortmannin for three days. Other samples were treated with 5- and 10-μmol/L wortmannin for three days, then recovered under normal culture conditions for another three days. DCFH-DA (25 μmol/L) was added to the culture and incubated at 10 °C for 1 h. Then, the cells were washed three times with sterile seawater to fully remove the DCFH-DA that did not enter the cells. ROS staining fluorescence was observed under 488-nm excitation light using a fluorescence microscope. Three fields in the middle of the thalli were randomly selected for each sample, and three biological replicates were prepared for each concentration.

2.6 Expression of *PI3K-AGC* pathway-related genes and NADPH oxidase genes

Thalli were collected after being treated with 0-, 5-, and 10-μmol/L wortmannin for 3 d in 500-mL flasks, and total RNA was extracted using a Plant RNA Kit (Omega, USA) after pre-cooling and grinding with liquid nitrogen. After the genomic DNA was removed, 1 μg of total RNA was used for reverse transcription using the PrimeScript™ RT reagent Kit with gDNA Eraser (Perfect Real Time) kit (TaKaRa), according to the manufacturer's protocol. Primers were designed according to the coding sequence (CDS) sequences of *PI3K-AGC* pathway-related genes (*PI3K*, *AGC*, *WEE1* kinase, and *CDKA*) and NADPH oxidase genes, using Oligo7 software (Table 1). After the PCR amplification of cDNA, the amplified fragment was transduced into the recombinant plasmid. The recombinant plasmids were sent to the Tsingke Company (Qingdao, China) for sequencing, and the sequencing results were compared using Snapgene software. The amplification efficiency and specificity of the primers were evaluated using a standard curve and a melting curve.

Table 1 List of primers used for quantitative PCR

Gene ID	Gene name	Primer sequence (5′→3′)
PyUBC-F	*UBC*	TCACAACGAGGATTTACCACC
PyUBC-R		GAGGAGCACCTTGGAAACG
py09517.t1-F	*CDKA*	GGTCCGACACACCCTGCC
py09517.t1-R		TCACCCGCTCGCCTCTCT
py03205.t1-F	*WEE1*	TACGCAGTCAAGCGAAGCAA
py03205.t1-R		CACGCACCGTGGTAACGC
py05971.t1-F	*PI3K*	GGCAAGAACCCTGAGAAGCA
py05971.t1-R		TGGTGACAACGCACGCATA
py04695.t1-F	*AGC*	GTCCTGCGAGTGGATGTGC
py04695.t1-R		CCCTGCGGTACGCCTTT
py00905.t1-F	*NOX*	CGTCTCACTTCACCGCTTTCT
py00905.t1-R		GACGAGCGTGCGGAGCT
py02269.t1-F	*NOX*	CGCTGGTGGTACTCCCTATGG
py02269.t1-R		TCGGTCAATGACGACGATGG
py02900.t1-F	*NOX*	GGGACAGTGACGAATGCGA
py02900.t1-R		GCGGACGAGTGGGAAGAGT
py07183.t1-F	*NOX*	GCGGGCCTTCCACTACACC
py07183.t1-R		AACACCATCTCCGACTCGT

ChamQTM SYBR Color qPCR Master Mix (Vazyme, China) was used for real-time quantitative PCR (qRT-PCR). The amplification system was used according to the instructions, and the PCR conditions were as follows: 95 °C for 1 min, 40 cycles at 95 °C for 15 s, 60 °C for 30 s, and 72 °C for 15 s. The amplification efficiency of qRT-PCR was detected by at least five serial ten-fold dilutions of plasmids containing the target cDNA. The reaction system was optimized to ensure that the melting curve had a single peak, and the primer amplification efficiency was between 95% and 105%. Then, 0-μmol/L wortmannin-treatment samples were used as the standard. Each treatment had three biological and three technical replicates. Under the correction of the internal reference gene (*pyUBC*), the relative expression of the target gene was calculated by the

Table 2 Homologous genes of the phosphatidylinositol signaling system in *P. yezoensis*

Gene name	Gene ID
Phosphatidylinositol-3 kinase (*PI3K*)	py05971.t1
Phosphatidylinositol 4-kinase (*PI4K*)	py02066.t1 and py03299.t1
Phosphatidylinositol-4-phosphate 5-kinase (*PIP5K*)	py08369.t1
Serine/threonine protein kinase (*AGC*)	py04695.t1
Inositol polyphosphate 5-phosphatase *INPP5D*	py04312.t1
Inositol polyphosphate 5-phosphatase *INPPL1*	py09662.t1
Inositol polyphosphate 5-phosphatase *INPP5B*	py06363.t1

$2^{-\Delta\Delta Ct}$ method and was analyzed by ANOVA using software SPSS.

3 RESULT

3.1 Phosphatidylinositol signalling-related genes in *P. yezoensis*

After a genome-wide survey and RefSeq non-redundant proteins (NR) database annotation, homologs relative to almost all PI signaling genes were found in the genome of *P. yezoensis*, indicating that the PI signaling pathway could be conserved in different eukaryotic kingdoms (Table 2; Fig.1).

The PI3K protein contained 868 amino acids with a deduced molecular weight (Mw) of 93.4 kDa and an isoelectric point (pI) of 7.21. Secondary structure prediction showed that this protein contained 39.75% alpha helix, 6.91% beta turn, and 34.79% random coils based on bioinformatics analysis. A phylogenetic tree based on the *PI3K* gene was constructed using MEGA-X with the ML method based on the *PI3K* gene amino acid sequence. The phylogenetic tree consisted of three large branches. The first branch contained two small clusters, the first of which was made up of fungi (such as *Saccharomyces cerevisiae* and *Fusarium oxysporum*), and the second was made up of higher plants (such as *Arabidopsis thaliana* and *Brassica napus*) and green algae (e.g., *Coccomyxa subellipsoidea*, *Pycnococcus provasolii*). In the second branch, *P. yezoensis* and red algae *Gracilariopsis chorda* had the highest homology and the closest evolutionary relationship. They gathered into a small cluster with the red algae *Porphyridium purpureum* and *Pyropia haitanensis*, and another small cluster composed of brown algae *Aureococcus anophagefferens*, golden algae *Emiliania huxleyi* CCMP1516, and green algae *Klebsormidium nitens*. The third branch of the phylogenetic tree was prokaryotic bacteria (e.g., Parcubacteria group bacterium GW2011_GWA2_42_14 and *Rhodovulum sulfidophilum*), which had the longest evolutionary distance. In addition, the *PI3K* of red algae was found to be more evolutionarily independent and may have its own characteristics (Fig.2).

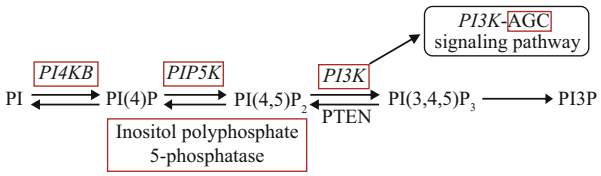

Fig.1 Pathway of phosphatidylinositol signaling system

Red box indicates genes found in *P. yezoensis*

3.2 NADPH oxidase genes and its cis-acting elements in *P. yezoensis*

In total, 11 NADPH oxidase genes were identified, of which 10 contained the NOX_Duox_like_FAD_NADP motif (Fig.3a), indicating that this motif plays an important role in the function of NADPH oxidase. In the action elements predicted in the promoter region of NADPH oxidase genes through the PlantCARE website, 1 927 cis-acting elements were obtained, of which 705 had clear functional annotations and could be divided into 18 different functional types. Among them, cis-acting elements related to stress response were the most common, accounting for 47.8%, and those related to hormone regulation accounted for 29.5% (Fig.3b). A total of 66 G-boxes and 9 W-boxes were identified. In addition, all 11 NADPH oxidase genes contained the 108 GC-motif, which is related to oxidative stress (Kaur and Pati, 2016).

3.3 Cell status and mitotic division measure

At concentrations of 5- and 10-μmol/L wortmannin, the cell morphology and autofluorescence of *P. yezoensis* thalli did not change noticeably (Fig.4a). Chlorophyll fluorescence imaging showed that there was no significant difference in the F_v/F_m values among the three groups (P>0.05) (Fig.4b). F_v/F_m

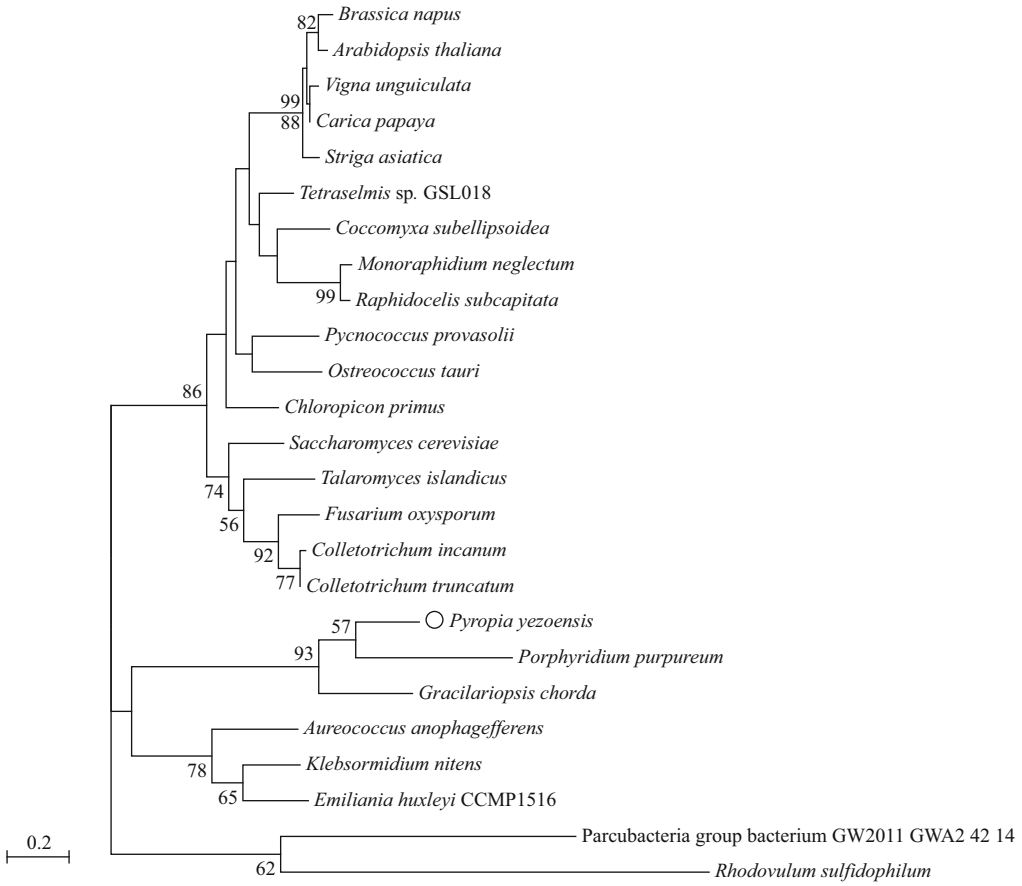

Fig.2 Maximum likelihood method tree based on PI3K amino acid

Numerical value of the branches of the phylogenetic tree represents genetic distance; node value represents test confidence (bootstrap=1 000); values less than 50 were hidden.

reflects the maximum photosynthetic potential of plants, which is known to decreases under stress (Maxwell and Johnson, 2000). In addition, no cell death was detected with 0.04% trypan blue (Fig.4a & c). The results indicated that wortmannin at the two concentrations did not change the morphology and photosynthetic physiology of the thalli nor caused the death of the thalli. Therefore, wortmannin at these concentrations could be used to study the function of PI3K in this experiment.

After 4 d of culture, significant differences were observed in the mitotic division rate of *P. yezoensis* in different wortmannin treatment groups ($P<0.05$). Mitotic division percentage was calculated as follows:

Mitotic division percentage=(EdU-labelled cells/ total number of cells)×100%.

The mitotic division percentage was 3.85%±0.64% in the 0-μmol/L group (Fig.5a & b), 1.23%±0.35% in the 5-μmol/L group (Fig.5c & d), and 0.31%±0.13% in the 10-μmol/L group (Fig.5e & f), suggesting that wortmannin inhibited mitotic division.

3.4 Reactive oxygen species detection

As shown in Fig.6, compared with the control group (Fig.6b), the ROS content decreased in the 5- and 10-μmol/L wortmannin-treated groups (Fig.6c & d), and increased after three days of recovery culture in normal seawater (Fig.6e & f). These results indicate that *PI3K* effectively regulated ROS production.

3.5 Expression levels detection of *PI3K-AGC* pathway-related genes and NADPH oxidase genes

After 3 d of wortmannin treatment, qRT-PCR was performed and the results showed that wortmannin effectively inhibited the expression of PI-related genes. As shown in Fig.7, after treatment with wortmannin, the expression levels of the *PI3K* gene (py05971.t1) and *AGC* gene (py04695.t1) decreased significantly in a dosage-dependent manner, thereby upregulating the expression of *WEE1* (py03205.t1), enhancing the inhibitory effect of *WEE1* on cyclin-dependent kinase A activity (*CDKA*, py09517.t1). The expression level of the *CDKA* gene decreased (Fig.7). Four NADPH

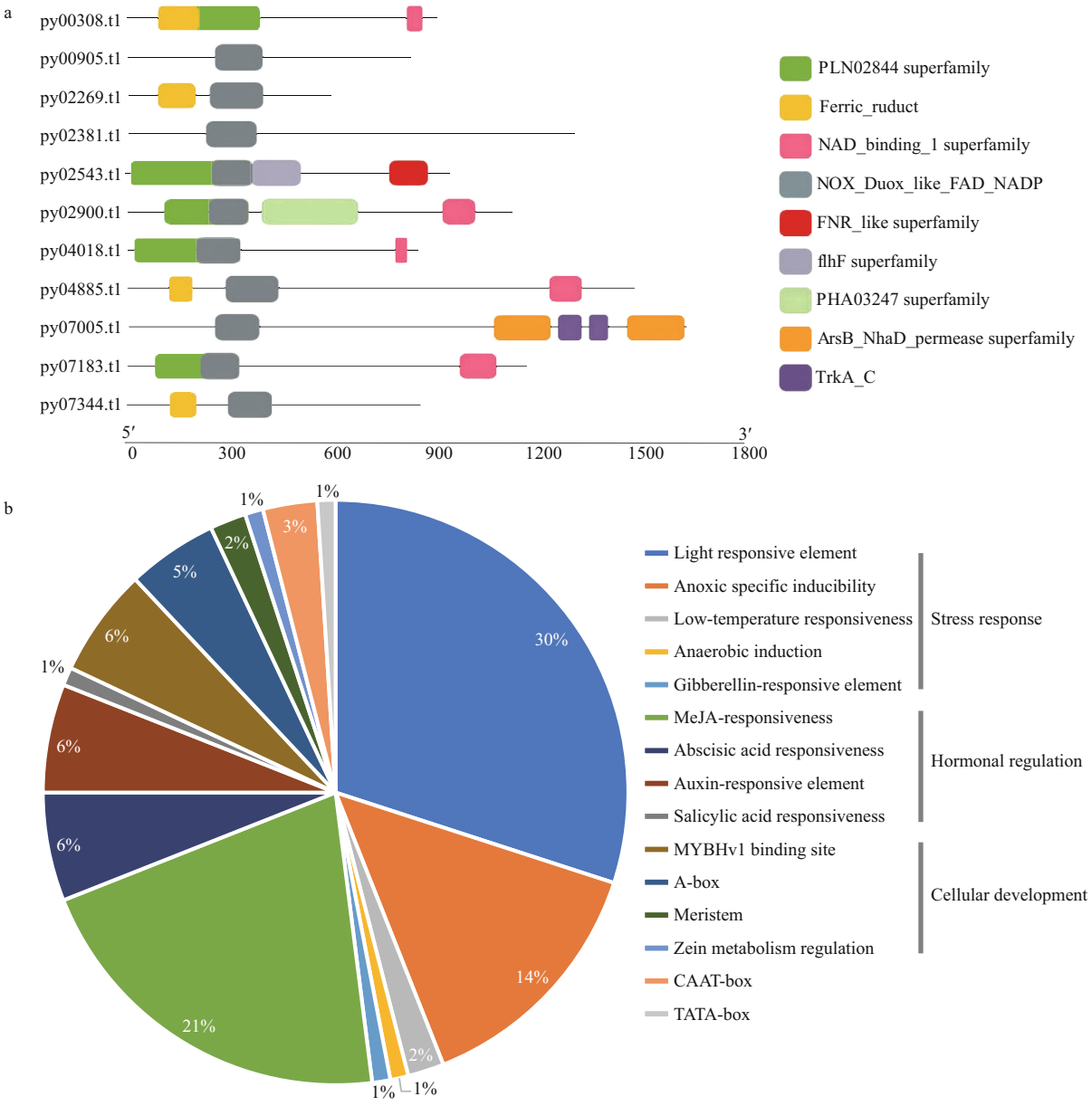

Fig.3 Bioanalysis of NADPH oxidase genes

a. analysis of NADPH oxidase proteins conserved motifs; b. the pie chart of identified motifs based on their biological functions in 2-kb upstream of NADPH oxidase genes in *P. yezoensis*.

oxidase genes with high expression under normal culture conditions were selected for verification of gene expression. Among them, py00905.t1 did not change significantly, whereas the expression of py02900.t1, py02269.t1, and py07183.t1 decreased with an increase in the inhibitor concentration (Fig.7).

4 DISCUSSION

As one of the central regulators of eukaryotic metabolism, the PI signaling system is widely present in eukaryotes (Heilmann, 2009). In animals and yeast, nuclear phosphoinositide regulates many processes, including vesicle transport, nuclear size, nuclear membrane reorganization, chromatin structure, DNA replication, DNA repair, transcription factor localization, transcription, RNA splicing, mRNA transport, and cell cycle progression (Dieck et al., 2012; Heilmann, 2016; Snider et al., 2017). In mammals, the PI signaling system plays a role in the orientation of the mitotic spindle and is involved in anaphase cell elongation (Cauvin and Echard, 2015). PI system enzymes have been identified in plant nuclei and are involved in DNA replication, chromatin remodeling, stress response, and hormone signaling (Dieck et al., 2012). Almost all homologous genes related to the PI signaling system were discovered in

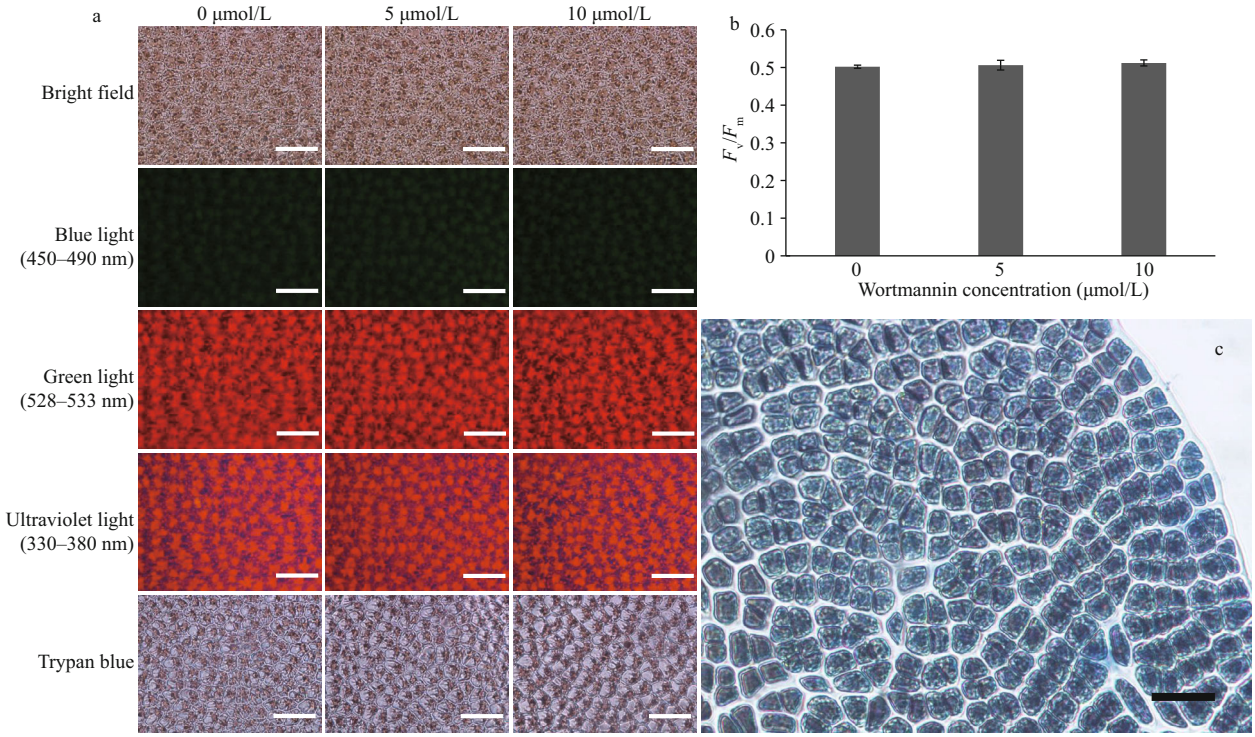

Fig.4 Cell state and viability under the treatment of different concentrations of wortmannin for three days

a. representative images of cell morphology and autofluorescence of *P. yezoensis* thalli treated with different concentrations of wortmannin; b. chlorophyll fluorescence parameter F_v/F_m of thalli under different concentrations of wortmannin ($P>0.05$); c. positive control for trypan blue-stained dead thalli. Scale bars: 50 μm, one-way ANOVA, $n=3$.

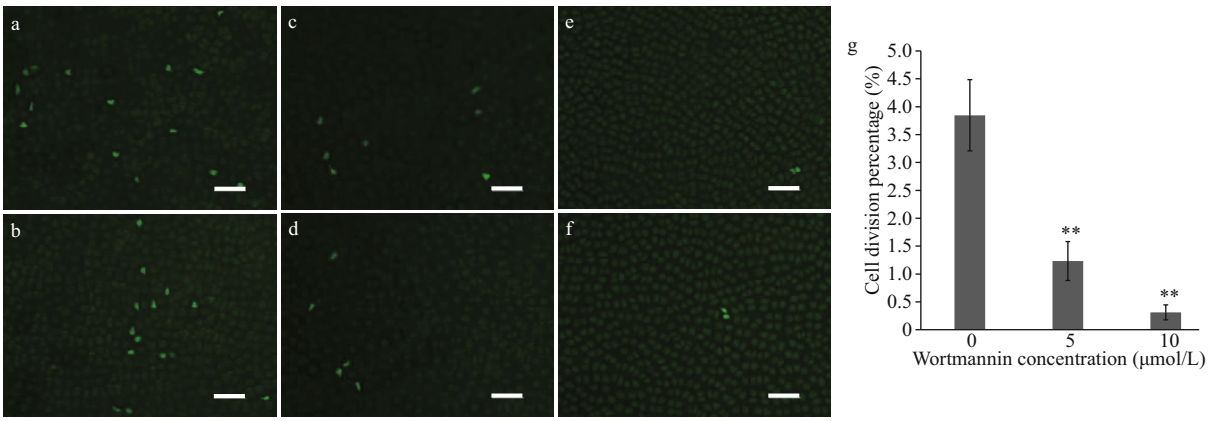

Fig.5 Mitotic division percentage in *P. yezoensis* treated with different concentrations (5 and 10 μmol/L) of wortmannin after EdU labelling for four days

a & b. vehicle (VEH); c & d. 5-μmol/L wortmannin; e & f. 10-μmol/L wortmannin; g. the bar graph of mitotic division percentage. Scale bars: 50 μm. **: $P<0.01$, one-way ANOVA, $n=3$.

P. yezoensis through this experiment, which indicated that the PI signaling pathway could be conserved in different eukaryotic kingdoms.

PI3K is involved in cell growth, morphogenesis, energy metabolism, vesicle transport, ROS regulation, and environmental adaptation in plants and algae (Liu et al., 2012; Cao et al., 2017). Therefore, *PI3K* is considered essential for the growth and development of eukaryotes; however, the importance of *PI3K* has not yet been elucidated in *P. yezoensis*. To provide direct evidence for the role of *PI3K* in mitotic division during the growth and development of *P. yezoensis*, wortmannin was used to treat the thalli. As a result, the mitotic division of *P. yezoensis* was found to be significantly inhibited in a dose-dependent manner: a dose of 5-μmol/L wortmannin reduced the mitotic division percentage by 68.1%, while 10-μmol/L wortmannin reduced the mitotic division percentage

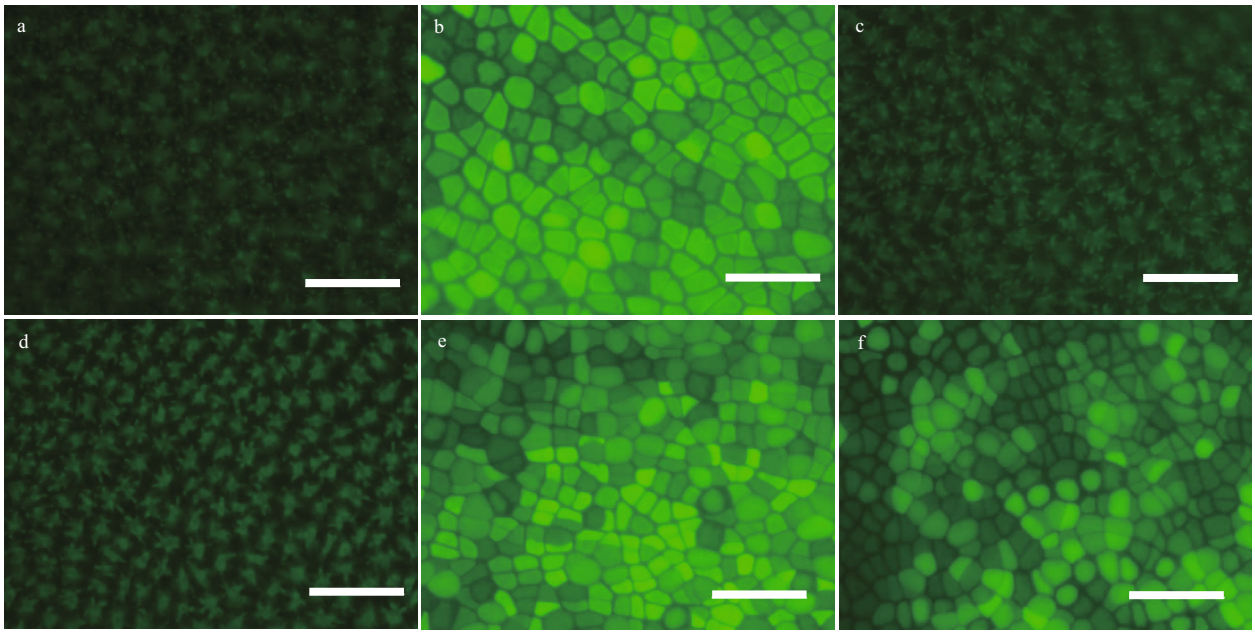

Fig.6 Content of ROS in *P. yezoensis* thalli that was wortmannin-treated for three days and recovered for another three days

a. autofluorescence of thalli cells; b. 0-μmol/L wortmannin; c. 5-μmol/L wortmannin; d. 10-μmol/L wortmannin; e. recovery after treatment with 5-μmol/L wortmannin; f. recovery after treatment with 10-μmol/L wortmannin. Scale bars: 50 μm.

by 91.9%. This result is in agreement with previous findings, where the treatment of sea urchin eggs with wortmannin was found to inhibit the activation of maturation promoting factor (MPF) and interfere with centrosome replication, thereby preventing mitotic spindle formation and resulting in cell cycle arrest (De Nadai et al., 1998). Another study found that wortmannin plays an important role in regulating nucleolus structure and function during wheat seed germination and inhibits wheat root growth and cell division (Ni and Zhang, 2014). To determine the precise mechanism underlying the decline in mitotic division, the expression of *PI3K-AGC* pathway-related genes was investigated, which have been previously shown to positively regulate the cell cycle (Wu et al., 2018). In this experiment, the inhibition of *PI3K* led to a decrease in downstream *AGC* gene expression, weakened the inhibitory effect of *AGC* on *WEE1*, and upregulated the expression of *WEE1*. Subsequently, the inhibitory effect of *WEE1* on *CDKA* activity was enhanced. The expression of *CDC2* homologous gene *CDKA* decreased. This could account for the decrease in the mitotic division percentage. The existing results only reflect the effect of inhibitors on gene transcription level, and the reason for other changes in gene expression under the action of wortmannin needs to be investigated further. Even so, the effect of *PI3K* on mitotic division in *P. yezoensis* has been preliminarily established.

In this study, when the thalli of *P. yezoensis* were treated with wortmannin, a specific inhibitor of *PI3K*, the ROS content was suppressed. ROS control and regulate a variety of biological processes, including growth, cell cycle, and development (Garg and Manchanda, 2009). Therefore, it is believed that *PI3K* stimulates the production of ROS and participates in the mechanism of ROS balance, thus acting on the growth and development of *P. yezoensis*. The release of ROS and its production sites depend on signal mechanisms, which involve the activity of cis-elements present in the upstream region of the target genes (such as NADPH oxidase genes) (Kaur and Pati, 2016). In *P. yezoensis*, the analysis of the upstream elements of NADPH oxidase genes revealed a total of 66 G-boxes and 9 W-boxes. Common components related to ROS include GCN4, TACCA/T-motif, and G-box, while the W-box is one of the main elements of ROS (Kaur and Pati, 2016). The G-box element (CACGTG) is widely distributed among plant genes and is known to participate in hormone signalling and play a role in light- and abscisic acid-mediated responses. Light and abscisic acid are related to many physiological and developmental processes, including seed germination and seedling development (Seo et al., 2006). The W-box interacts with members of the WRKY transcription factor family, which is known to play a role in biotic and abiotic stress, leaf senescence, and

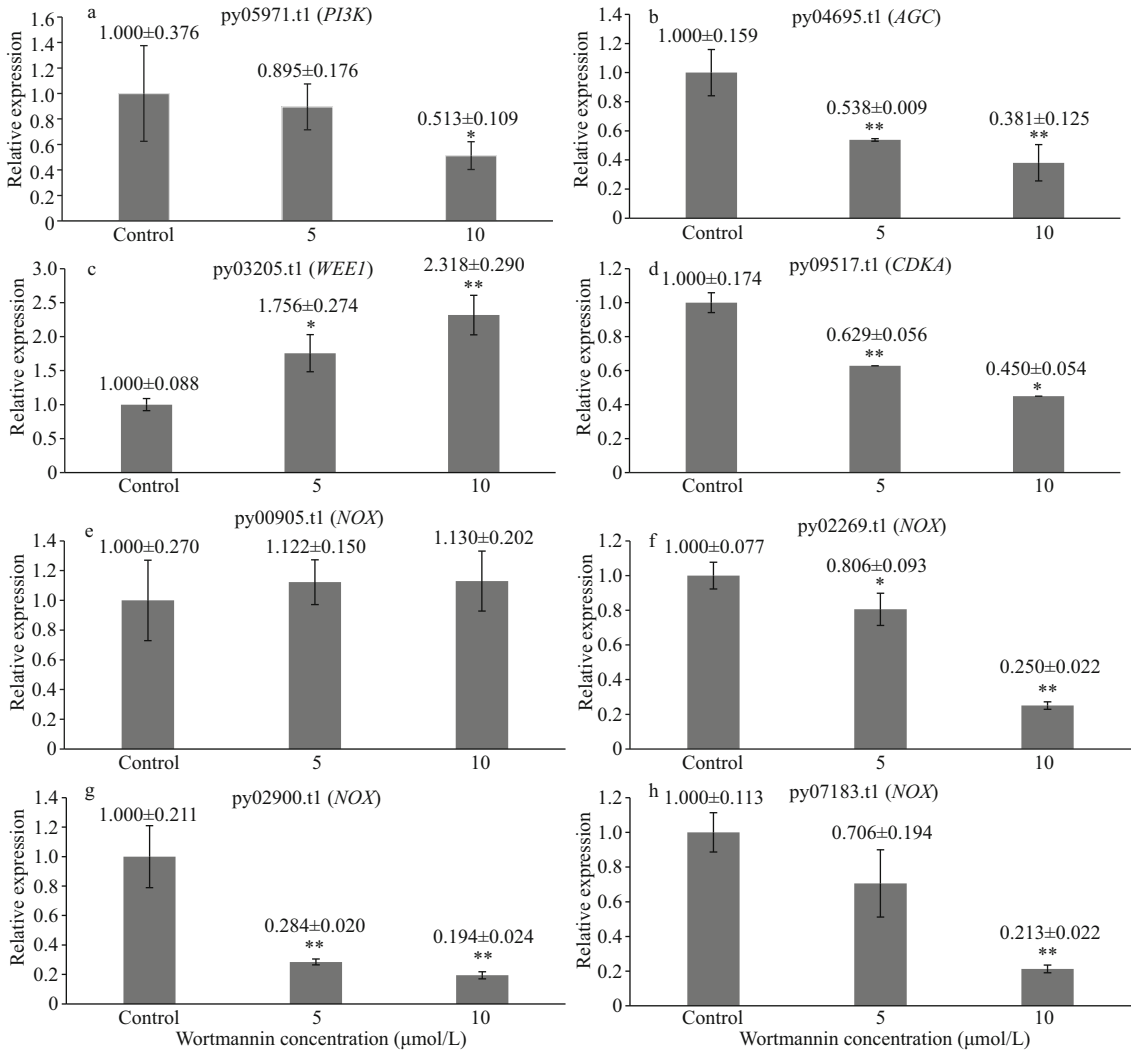

Fig.7 Expression changing of PI-related genes after wortmannin treatment for three days

a. expression level of *PI3K* gene after wortmannin treatment; b. expression level of *AGC* gene after wortmannin treatment; c. expression level of *WEE1* gene after wortmannin treatment; d. expression level of *CDKA* gene after wortmannin treatment; e–h. expression level of *NOX* gene after wortmannin treatment. *: $P<0.05$; **: $P<0.01$, one-way ANOVA, $n=3$.

seed development (Rushton et al., 2010). Therefore, NADPH oxidase gene expression could be regulated by the G-box and W-box elements in the growth and development of *P. yezoensis*. Taken together, these results suggest that *PI3K* plays a role in ROS production by influencing the expression of NADPH oxidase genes in *P. yezoensis*. In plants, the hypothesis that *PI3K* activates NADPH oxidase by regulating the transport of RAC1 protein from the cytoplasm to the plasma membrane has been proposed previously (Liu et al., 2012). However, the mechanism by which *PI3K* regulates the expression and activity of NADPH oxidase in *P. yezoensis* requires further investigation.

5 CONCLUSION

PI3K was conserved in *P. yezoensis* and functioned in similar to those in other animals and plants, showing dual effects in regulating cell division and determining ROS levels. In addition, the PI signaling system played an important role in growth and development of *P. yezoensis*. The *PI3K*-*AGC* pathway was a key factor in promoting cell division. *PI3K* weakened the expression of the downstream *AGC* gene, and further upregulated the expression of *WEE1*. *CDKA* activity was inhibited and the expression of *CDKA* was decreased, both of which led to cell cycle arrest. *PI3K* also regulated the ROS homeostasis potentially by promoting the gene expression of NADPH oxidase (*NOX*), which codes for key enzymes in ROS production.

However, this study was solely based on the detection of key genes at the expression level, more

complex regulatory network between genes and gene products, including their regulation mechanisms, will be clarified in future studies.

6 DATA AVAILABILITY STATEMENT

The data generated and/or analyzed during the current study are available from the corresponding author upon reasonable request.

References

Alvarez B, Garrido E, Garcia-Sanz J A, Carrera A C. 2003. Phosphoinositide 3-kinase activation regulates cell division time by coordinated control of cell mass and cell cycle progression rate. *Journal of Biological Chemistry*, **278**(29): 26466-26473, https://doi.org/10.1074/jbc.M300663200.

Aranda A, Sequedo L, Tolosa L, Quintas G, Burello E, Castell J V, Gombau L. 2013. Dichloro-dihydro-fluorescein diacetate (DCFH-DA) assay: a quantitative method for oxidative stress assessment of nanoparticle-treated cells. *Toxicology in Vitro*, **27**(2): 954-963, https://doi.org/10.1016/j.tiv.2013.01.016.

Blouin N A, Brodie J A, Grossman A C, Xu P, Brawley S H. 2011. *Porphyra*: a marine crop shaped by stress. *Trends in Plant Science*, **16**(1): 29-37, https://doi.org/10.1016/j.tplants.2010.10.004.

Campa C C, Martini M, De Santis M C, Hirsch E. 2015. How PI3K-derived lipids control cell division. *Frontiers in Cell and Developmental Biology*, **3**: 61, https://doi.org/10.3389/fcell.2015.00061.

Cao H, Ni X L, Zhang C Y, Shi W S, Xu Y X, Yan Y M, Zhang F X. 2017. Alterations in the proteome of wheat primary roots after wortmannin application during seed germination. *Acta Physiologiae Plantarum*, **39**(10): 223, https://doi.org/10.1007/s11738-017-2511-9.

Cauvin C, Echard A. 2015. Phosphoinositides: lipids with informative heads and mastermind functions in cell division. *Biochimica et Biophysica Acta* (*BBA*)-*Molecular and Cell Biology of Lipids*, **1851**(6): 832-843, https://doi.org/10.1016/j.bbalip.2014.10.013.

Chen C J, Chen H, Zhang Y, Thomas H R, Frank M H, He Y H, Xia R. 2020. TBtools: An integrative toolkit developed for interactive analyses of big biological data. *Molecular Plant*, **13**(8): 1194-1202, https://doi.org/10.1016/j.molp.2020.06.009.

Dangi S, Cha H, Shapiro P. 2003. Requirement for phosphatidylinositol-3 kinase activity during progression through S-phase and entry into mitosis. *Cellular Signalling*, **15**(7): 667-675, https://doi.org/10.1016/S0898-6568(03)00002-0.

De Nadai C, Huitorel P, Chiri S, Ciapa B. 1998. Effect of wortmannin, an inhibitor of phosphatidylinositol 3-kinase, on the first mitotic divisions of the fertilized sea urchin egg. *Journal of Cell Science*, **111**(Pt 17): 2507-2518, https://doi.org/10.1016/S1357-2725(98)00066-1.

Dieck C B, Boss W F, Perera I Y. 2012. A role for phosphoinositides in regulating plant nuclear functions. *Frontiers in Plant Science*, **3**: 50, https://doi.org/10.3389/fpls.2012.00050.

Elge S, Brearley C, Xia H J, Kehr J L, Xue H W, Mueller-Roeber B. 2001. An *Arabidopsis* inositol phospholipid kinase strongly expressed in procambial cells: Synthesis of PtdIns(4,5)P_2 and PtdIns(3,4,5)P_3 in insect cells by 5-phosphorylation of precursors. *The Plant Journal*, **26**(6): 561-571, https://doi.org/10.1046/j.1365-313x.2001.01051.x.

Foreman J, Demidchik V, Bothwell J H F, Mylona P, Miedema H, Torres M A, Linstead P, Costa S, Brownlee C, Jones J D G, Davies J M, Dolan L. 2003. Reactive oxygen species produced by NADPH oxidase regulate plant cell growth. *Nature*, **422**(6930): 442-446, https://doi.org/10.1038/nature01485.

Fujinami R, Yamada T, Nakajima A, Takagi S, Idogawa A, Kawakami E, Tsutsumi M, Imaichi R. 2017. Root apical meristem diversity in extant lycophytes and implications for root origins. *New Phytologist*, **215**(3): 1210-1220, https://doi.org/10.1111/nph.14630.

Garg N, Manchanda G. 2009. ROS generation in plants: boon or bane? *Plant Biosystems*: *An International Journal Dealing with all Aspects of Plant Biology*, **143**(1): 81-96, https://doi.org/10.1080/11263500802633626.

Hakeem K R, Rehman R U, Tahir I. 2014. Plant Signaling: Understanding the Molecular Crosstalk. Springer, New Delhi. 355p.

Heilmann I. 2009. Using genetic tools to understand plant phosphoinositide signalling. *Trends in Plant Science*, **14**(3): 171-179, https://doi.org/10.1016/j.tplants.2008.12.002.

Heilmann I. 2016. Phosphoinositide signaling in plant development. *Development*, **143**(12): 2044-2055, https://doi.org/10.1242/dev.136432.

Joo J H, Yoo H J, Hwang I, Lee J S, Nam K H, Bae Y S. 2005. Auxin-induced reactive oxygen species production requires the activation of phosphatidylinositol 3-kinase. *FEBS Letters*, **579**(5): 1243-1248, https://doi.org/10.1016/j.febslet.2005.01.018.

Katayama K, Fujita N, Tsuruo T. 2005. Akt/Protein kinase B-dependent phosphorylation and Inactivation of WEE1Hu promote cell cycle progression at G_2/M transition. *Molecular and Cellular Biology*, **25**(13): 5725-5737, https://doi.org/10.1128/MCB.25.13.5725-5737.2005.

Kaur G, Pati P K. 2016. Analysis of cis-acting Regulatory elements of respiratory burst oxidase homolog (*Rboh*) gene families in *Arabidopsis* and rice provides clues for their diverse functions. *Computational Biology and Chemistry*, **62**: 104-118, https://doi.org/10.1016/j.compbiolchem.2016.04.002.

Lee Y, Bak G, Choi Y, Chuang W I, Cho H T, Lee Y. 2008. Roles of phosphatidylinositol 3-kinase in root hair growth. *Plant Physiology*, **147**(2): 624-635, https://doi.org/10.1104/pp.108.117341.

Lee Y, Munnik T, Lee Y. 2010. Plant phosphatidylinositol 3-kinase. *In*: Munnik T ed. Lipid Signaling in Plants.

Springer, Berlin. p.95-106.

Li L, Saga N, Mikami K. 2008. Phosphatidylinositol 3-kinase activity and asymmetrical accumulation of F-actin are necessary for establishment of cell polarity in the early development of monospores from the marine red alga *Porphyra yezoensis*. *Journal of Experimental Botany*, **59**(13): 3575-3586, https://doi.org/10.1093/jxb/ern207.

Liu J, Zhou J, Xing D. 2012. Phosphatidylinositol 3-kinase plays a vital role in regulation of rice seed vigor via altering NADPH oxidase activity. *PLoS One*, **7**(3): e33817, https://doi.org/10.1371/journal.pone.0033817.

Livanos P, Apostolakos P, Galatis B. 2012. Plant cell division: ROS homeostasis is required. *Plant Signaling & Behavior*, **7**(7): 771-778, https://doi.org/10.4161/psb.20530.

Marqués M, Kumar A, Poveda A M, Zuluaga S, Hernández C, Jackson S, Pasero P, Carrera A C, Verma I M. 2009. Specific function of phosphoinositide 3-kinase β in the control of DNA replication. *Proceedings of the National Academy of Sciences of the United States of America*, **106**(18): 7525-7530, https://doi.org/10.1073/pnas.0812000106.

Maxwell K, Johnson G N. 2000. Chlorophyll fluorescence—a practical guide. *Journal of Experimental Botany*, **51**: 659-668, https://doi.org/10.1093/jexbot/51.345.659.

Ni X L, Zhang F X. 2014. PI3K is involved in nucleolar structure and function on root-tip meristematic cells of *Triticum aestivum* L. *Acta Histochemica*, **116**(5): 838-843, https://doi.org/10.1016/j.acthis.2014.02.004.

Powis G, Bonjouklian R, Berggren M M, Gallegos A, Abraham R, Ashendel C, Zalkow L, Matter W F, Dodge J, Grindey G. 1994. Wortmannin, a potent and selective inhibitor of phosphatidylinositol-3-kinase. *Cancer Research*, **54**(9): 2419-2423, https://doi.org/10.1007/s002620050075.

Ramanan R, Tran Q G, Cho D H, Jung J E, Kim B H, Shin S Y, Choi S H, Liu K H, Kim D S, Lee S J, Crespo J L, Lee H G, Oh H M, Kim H S. 2018. The ancient phosphatidylinositol 3-kinase signaling system is a master regulator of energy and carbon metabolism in algae. *Plant Physiology*, **177**(3): 1050-1065, https://doi.org/10.1104/pp.17.01780.

Rastogi R P, Singh S P, Häder D P, Sinha R P. 2010. Detection of reactive oxygen species (ROS) by the oxidant-sensing probe 2', 7'-dichlorodihydrofluorescein diacetate in the cyanobacterium *Anabaena variabilis* PCC 7937. *Biochemical and Biophysical Research Communications*, **397**(3): 603-607, https://doi.org/10.1016/j.bbrc.2010.06.006.

Rushton P J, Somssich I E, Ringler P, Shen Q X J. 2010. WRKY transcription factors. *Trends in Plant Science*, **15**(5): 247-258, https://doi.org/10.1016/j.tplants.2010.02.006.

Sato-Izawa K, Nakaba S, Tamura K, Yamagishi Y, Nakano Y, Nishikubo N, Kawai S, Kajita S, Ashikari M, Funada R, Katayama Y, Kitano H. 2012. *DWARF50* (*D50*), a rice (*Oryza sativa* L.) gene encoding inositol polyphosphate 5-phosphatase, is required for proper development of intercalary meristem. *Plant*, *Cell & Environment*, **35**(11): 2031-2044, https://doi.org/10.1111/j.1365-3040.2012.02534.x.

Seo M, Hanada A, Kuwahara A, Endo A, Okamoto M, Yamauchi Y, North H, Marion-Poll A, Sun T P, Koshiba T, Kamiya Y, Yamaguchi S, Nambara E. 2006. Regulation of hormone metabolism in *Arabidopsis* seeds: phytochrome regulation of abscisic acid metabolism and abscisic acid regulation of gibberellin metabolism. *The Plant Journal*, **48**(3):354-366,https://doi.org/10.1111/j.1365-313X.2006.02881.x.

Shigaki T, Bhattacharyya M K. 2002. Nutrients induce an increase in inositol 1,4,5-trisphosphate in soybean cells: implication for the involvement of phosphoinositide-specific phospholipase C in DNA synthesis. *Plant Biology*, **4**(1): 53-61, https://doi.org/10.1055/s-2002-20436.

Snider C E, Willet A H, Chen J S, Arpağ G, Zanic M, Gould K L. 2017. Phosphoinositide-mediated ring anchoring resists perpendicular forces to promote medial cytokinesis. *The Journal of Cell Biology*, **216**(10): 3041-3050, https://doi.org/10.1083/jcb.201705070.

Tang L, Qiu L P, Liu C, Du G Y, Mo Z L, Tang X H, Mao Y X. 2019. Transcriptomic insights into innate immunity responding to red rot disease in red alga *Pyropia yezoensis*. *International Journal of Molecular Sciences*, **20**(23): 5970, https://doi.org/10.3390/ijms20235970.

Wang D M, Yu X Z, Xu K P, Bi G Q, Cao M, Zelzion E, Fu C X, Sun P P, Liu Y, Kong F N, Du G Y, Tang X H, Yang R J, Wang J H, Tang L, Wang L, Zhao Y J, Ge Y, Zhuang Y Y, Mo Z L, Chen Y, Gao T, Guan X W, Chen R, Qu W H, Sun B, Bhattacharya D, Mao Y X. 2020. *Pyropia yezoensis* genome reveals diverse mechanisms of carbon acquisition in the intertidal environment. *Nature Communications*, **11**(1): 4028, https://doi.org/10.1038/s41467-020-17689-1.

Wang Y, Chu Y J, Xue H W. 2012. Inositol polyphosphate 5-phosphatase-controlled Ins $(1,4,5)P_3/Ca^{2+}$ is crucial for maintaining pollen dormancy and regulating early germination of pollen. *Development*, **139**(12): 2221-2233, https://doi.org/10.1242/dev.081224.

Wu S F, Wang S Z, Gao F, Li L Y, Zheng S Y, Yung W K A, Koul D. 2018. Activation of WEE1 confers resistance to PI3K inhibition in Glioblastoma. *Neuro-Oncology*, **20**(1): 78-91, https://doi.org/10.1093/neuonc/nox128.

Xu X J, Liu X Y, Zhang Y. 2018. Osthole inhibits gastric cancer cell proliferation through regulation of PI3K/AKT. *PLoS One*, **13**(3): e0193449, https://doi.org/10.1371/journal.pone.0193449.

Yamada M, Han X W, Benfey P N. 2020. RGF1 controls root meristem size through ROS signalling. *Nature*, **577**(7788): 85-88, https://doi.org/10.1038/s41586-019-1819-6.